ChemPubSoc Europe

DOI: 10.1002/ejic.201701280

EurJIC European Journal of Inorganic Chemistry

Microreview

Oxidative Cracking

Catalytic Oxidative Cracking of Light Alkanes to Alkenes

Cassia Boyadjian*[a] and Leon Lefferts[b]

Abstract: A review on the catalytic oxidative cracking of light alkanes to alkenes is presented as an alternative route to steam cracking for production of alkenes. Catalytic oxidative cracking is a combination of heterogeneous and homogeneous reactions; the reaction is initiated on the catalyst surface followed by thermal gas phase cracking. The review focuses on the catalytic generation of alkyl radicals at moderate temperatures (550–650 °C) using the Li/MgO system. Comparison with other catalyst systems such as Li/Y_2O_3, Au/La_2O_3, Au-SCZ, BiOCl, B_2O_3/Al_2O_3, Co-N/Al_2O_3 and Pt/Al_2O_3 monoliths is included. Gold supported on sulfated ceria-zirconia catalyst (Au-SCZ) is concluded to be a promising catalyst for further study. In addition to catalytic initiation of radicals, the review discusses alkyl generation using non-equilibrium plasma. Plasma-catalysis in oxidative cracking induces synergy effects and introduces significant improvement in yields of alkenes; however, further understanding of plasma chemistry needs to be elaborated. Minimizing CO_2 production and maximizing yields of valuable C_2–C_4 alkenes remains the bottleneck for the commercialization of oxidative cracking process. Future research should focus on reactor design and on developing optimized reactor-catalyst systems.

1. Introduction

Catalytic oxidative cracking has received considerable interest in the past years as an alternative to steam cracking for the production of light alkenes. Light alkenes i.e. ethene and propene are the building blocks of the petrochemical industry and the basis for a broad range of consumables. The annual production for ethene and propene is roughly 1.5×10^8 t and 8×10^7 t, respectively.[1] Yet, due to a rapidly growing world population, the demand for these alkenes is increasing tremendously,[2] with demand for propene growing stronger than that of ethene.[3,4]

Besides some commercialized on-purpose alkene technologies, (dehydrogenation and methanol to alkenes),[5] steam cracking remains today the major route for the production of light alkenes. However, it is a very energy intensive process, which makes it economically and ecologically less attractive. It is reported that the pyrolysis section of a naphtha steam cracker alone consumes approximately 65 % of the total process energy required and generates approximately 75 % of the total exergy loss.[6] Consequently, the process is accompanied by high emissions of CO_2 as a result of fuel combustion. More-

[a] *Department of Chemical and Petroleum Engineering, Maroun Semaan Faculty of Engineering and Architecture, American University of Beirut, P.O.Box 11-0236, Riad El-Solh, Beirut 1107 2020, Lebanon*
E-mail: cb30@aub.edu.lb
http://aub.edu.lb/fea/chen/Pages/default.aspx
[b] *Catalytic Processes and Materials, Mesa+ Institute for Nanotechnology, University of Twente,*
Drienerlolaan 5, 7522 NB Enschede, the Netherlands
E-mail: l.lefferts@utwente.nl
https://www.utwente.nl/en/tnw/cpm/
ORCID(s) from the author(s) for this article is/are available on the WWW under https://doi.org/10.1002/ejic.201701280.

Cassia Boyadjian was born in 1978 in Beirut, Lebanon. She has a master's degree (2005) in process engineering and PhD (2010) in heterogeneous catalysis from the University of Twente in the Netherlands. Her PhD work was performed at the catalytic processes and materials group, on catalytic cracking of n-hexane, as an alternative route to steam cracking for production of light alkenes. In 2011–2013 she worked at BASF in Ludwigshafen as research scientist on petrochemical catalysts to carry out research work on catalytic oxidative cracking of naphtha. In 2013–2014 she worked at BASF-Antwerp as process engineer. In 2014 she joined the American University of Beirut as assistant professor of chemical engineering. Her research interests are in catalytic conversion of waste and renewable carbon sources into chemicals and fuel.

Leon Lefferts (1960) was trained as a chemical engineer at the University of Twente and received his PhD in 1987. The Royal Dutch Chemical Society awarded his thesis with the Catalysis Prize of the section Catalysis. He continued to specialize on heterogeneous catalysis and joined the DSM Research laboratories, working on catalyst characterization, hydrogenation, slurry phase catalysis, carbon-supported metals, and kinetics. He was appointed full professor "Catalytic Processes and Materials" at the University of Twente in 1999. He has been visiting professor at Tokyo Institute of Technology and holds a visiting professorship at Aalto University. His research interests within the field of applied heterogeneous catalysis include activation of stable molecules (e.g. CH_4, CO_2, H_2O and N_2) heterogeneous catalysis in liquid phase, and catalysis for bio-based molecules to fuels and chemicals. He (co-)authored over 220 peer-reviewed scientific publications and three patents.

over, the shift to lighter feedstocks in steam crackers[5] makes the production capacities of C_3–C_4 alkenes from this process insufficient to meet the growing demands of these alkenes. This urges the presence of *on-purpose* alkene technologies. Considering these issues, although being state of art technology, researchers have been looking in the past years for alternative processes to steam cracking.

Catalytic oxidative cracking is conceptually a potential alternative process to steam cracking and brings the following advantages: (1) autothermal operation; reaction in presence of oxygen is exothermic and generates in-situ heat for endothermic cracking reactions. This minimizes external heat input and reduces investment costs of utilities. (2) Cofeeding oxygen helps to minimize the extent of coke formation and (3) the presence of catalyst enables activation of cracking reactions at lower temperatures, allowing further tuning of selectivity to alkenes.

In, non-catalytic, oxidative cracking of alkanes, there is an agreement on that presence of oxygen in the feed alters reaction thermodynamics, accelerating reaction rate and alkane conversions. Moreover, oxygen inhibits the formation of heavy products, which are precursors for tar and soot formation.[7–10] For the cracking of *n*-hexane at 650 °C,[9] *n*-hexane conversion and yield of alkenes in absence of oxygen are 2.3 and 1.4 wt.-%, respectively, while in oxidative cracking, they reach 72.2 and 39.1 wt.-%, respectively. Oxidative cracking results in slightly lower alkene selectivities than non-oxidative cracking due to CO_x formation. High CO/CO_2 ratios indicates the dominancy of partial oxidation of *n*-hexane over total oxidation.

It is well known that thermal cracking is initiated by C–C bond scission and radical formation, which later propagates in gas phase forming cracking products.[11] In gas phase oxidative cracking, there is clear evidence that oxygen participates in the initiation of the chain reaction and partially oxidizes some of the alkane to form carbon monoxide and water, releasing heat necessary for propagation reaction of the remaining hexane, i.e. β-decomposition of free radicals formed.[9]

The use of catalyst in oxidative cracking reactions is justified by its role in initiating cracking reactions at temperatures lower than those required for non-catalytic reactions. At these low temperatures, the active catalyst initiates cracking reactions when extent of gas phase initiation remains small. After initiation however, thermal cracking in gas phase is a dominant reaction route. Catalytic oxidative cracking, is hence, a combination of heterogeneous (catalytic) and homogeneous (gas phase) reactions. Additionally, the catalyst helps tuning the product selectivity towards the formation of light alkenes.[12–16] In the absence of the catalyst the formation of higher hydrocarbons (alkanes, aromatics) are common. The presence of the catalyst is thus crucial in improving alkene yields at conditions when gas phase cracking would result in minimal alkene formation. For example, catalytic cracking of hexane over Li/MgO catalyst at 575 °C, results in 17 wt.-% yield of C_2–C_4 alkenes (28 wt.-% C_6 conversion and 60 wt.-% selectivity to C_2–C_4 alkenes) while non-catalytic cracking results only in 1 wt.-% yield of alkenes.[14] It is worth mentioning that in catalytic oxidative cracking, total oxidation reactions dominate over partial oxidation leading to CO_2 formation. CO_2 formation is unavoidable in oxidative cracking and has always been the bottleneck, preventing commercialization of this process.[17]

Researchers have investigated different catalytic systems for the oxidative cracking of light alkanes (C_1–C_5). In all these processes, the catalyst plays a significant role in initiation and acceleration of the cracking reaction. The initiation mechanism of cracking in these reactions very much depends on the nature of the active sites of the catalyst. Basically two mechanisms are reported:

(1) Surface initiation by hydrogen abstraction from the alkane and formation of alkyl species/radicals which further undergo β-scission reaction in gas phase to yield cracking products. Catalysts systems reported are: (1) Alkali, alkaline earth, and rare earth oxides such as Li/MgO,[12–21] Li/La_2O_3 and Li/Y_2O_3,[8,22–25] (2) gold-containing catalysts such as Au/La_2O_3[26] and gold supported on sulfated ceria-zirconia (Au-SCZ),[27] (3) nitrogen-containing cobalt supported on alumina,[28,29] (4) boria catalysts,[30–32] and (5) oxychlorides.[33] Molybdena and vanadia-based catalysts are mainly reported for oxidative dehydrogenation reactions and will not be discussed here.[34–40] Li/MgO is repeatedly reported in literature for the oxidative cracking of lower alkanes. At the University of Twente, we have conducted extensive work studying moderate and low temperature alkyl radical generation using Li/MgO[12–19] and combined plasma-Li/MgO systems;[41–45] in the oxidative cracking of propane, butane and *n*-hexane.

(2) Surface catalyzed oxidation reactions followed by gas phase thermal cracking. This is a common mechanism when Pt coated monoliths are used as described by Schmidt and co-workers in the oxidative cracking of alkanes at short contact times of milliseconds.[46–54] In this review, we will present and discuss the performance of these various catalyst systems for the oxidative cracking of alkanes. We will emphasize however on work done at the University of Twente on the Li/MgO system, describing active site, mechanism and performance, in addition to application of non-equilibrium plasma for enhanced radical generation. In addition to catalyst systems, the review will present an insight on the economic feasibility of the process.

2. Catalyst Systems for Oxidative Cracking

2.1. Li/MgO

Magnesium oxide exhibits poor activity and selectivity to alkenes in the oxidative cracking of lower alkanes.[55] However, as the case with the rare earth oxides, Li promotion of MgO results in significant improvement in catalyst performance.[55–57] Li/MgO has been extensively studied in literature for the oxidative conversion of alkanes; oxidative coupling of methane[58–62] and oxidative dehydrogenation/cracking of ethane,[34,63] propane, butane and hexane.[12–19] Usually, alkane conversion increases with the increase in the carbon chain length, due to the decrease in the C–H bond strength. For example, at 600 °C, catalytic cracking of *n*-propane over 1 %Li/MgO results in 33 wt.-% conversion of propane and 56 wt.-% selectivity to alkenes (18 wt.-% yields of alkenes).[12] At the same temperature, cata-

lytic cracking of *n*-hexane, results in 36 wt.-% conversion and 61 wt.-% selectivity to C_2–C_4 alkenes (22 wt.-% yields of alkenes).[14]

2.1.1 Active Site and Cracking Mechanism

There is a general agreement in literature, based on the extensive spectroscopic work of Knözinger and co-workers[64,65] and recent literature,[66,67] that the catalytic function of MgO is connected to defect sites and is not a property of the MgO phase. MgO itself is a poor oxidation catalyst due to the lack of mobile electrons which stay trapped at the defect sites. Low coordinated $Mg^{2+}{}_{LC}O^{2-}{}_{LC}$ sites at steps and corners are believed to be the active sites for hydrogen abstraction from the alkane during oxidative cracking reactions.[56,64,65]

As far as concerning the lithium promotion of MgO, there is clear evidence based on the work of Knözinger[55] and more recently Lefferts and co-workers from University of Twente[68,69] and Schlögl and co-workers[56,57,66,67] from Frits Haber Institute and Hamboldt University, that lithium ions effectively alter morphology of MgO leading to better performance for oxidative cracking reactions.

Two claims are reported in literature explaining the nature of the active sites of Li/MgO catalyst. The first claim is presented by Lunsford and co-workers, who extensively studied the Li/MgO system for the oxidative coupling of methane.[58,59] They attributed catalyst activity in methane activation to $[Li^+O^-]$ sites of the catalyst.[58] The mechanism for the formation of the $[Li^+O^-]$ sites was described based on the proposition made earlier by Abraham and co-workers.[70,71] Upon thermal treatment of MgO doped with Li, Li^+ ions diffuse and substitute Mg^{2+} cations [Equation (1)]. The excess of the cations on the MgO matrix leads to the formation of oxygen vacancies which in the presence of gas phase oxygen at high temperatures, result in O^{2-} ions and $[Li^+O^-]$ centers [Equation (2)].

This process is expressed by the following equation, V_o denotes oxygen vacancy:[58]

$$Li_2O + 2Mg^{2+}_{Mg} + O^{2-}_O \rightarrow 2Li^{2+}_{Mg} + V_O + 2Mg \quad (1)$$

$$2Li^+O^{2-} + Vo + 1/2O_2 \Leftrightarrow 2Li^+O^- + O^{2-} \quad (2)$$

Alternatively, Trionfetti et al. reported on the sol-gel method for the preparation of the Li/MgO.[68,69] With this method incorporation of Li in magnesia is achieved under milder conditions (during sol–gel transformation), avoiding the need to calcine the catalyst at very high temperatures. Thus, compared to the catalyst prepared via the conventional impregnation route, the sol-gel prepared catalyst exhibits both higher surface area and higher concentration of active sites.

The reaction model for OCM as proposed by Lunsford and co-workers is as the following:[58]

At first $CH_3^{\cdot}$ radicals are formed from reaction of CH_4 with $[O^-]$ sites of $[Li^+O^-]$.

$$CH_4 + Li^+O^- \rightarrow Li^+OH^- + CH_3^{\cdot} \quad (3)$$

The methyl radical is released to gas phase and follows a series of reactions: (1) Coupling with another methyl radical to form ethane [Equation (4)] and (2) reaction with gas phase oxygen to form methylperoxy radical which acts as chain propagator and accelerates gas phase chemistry [Equation (5)].

$$2CH_3^{\cdot} \rightarrow C_2H_6 \quad (4)$$

$$CH_3^{\cdot} + O_2 \rightarrow CH_3O_2^{\cdot} \quad (5)$$

Ethane formed, can further interact with oxygen to form ethyl radical which reacts in gas phase to form ethene:

$$C_2H_6 + O_s^- \rightarrow C_2H_5^{\cdot} + OH^- \quad (6)$$

$$C_2H_5^{\cdot} + O^{2-} \rightarrow OC_2H_5^- + e^- \quad (7)$$

$$OC_2H_5^- \rightarrow C_2H_4 + OH^- \quad (8)$$

The hypothesis by Lunsford concerning the $[Li^+O^-]$ active sites in Li/MgO was generally accepted for a long time, until it was recently questioned by Kwapien et al.[57] This research group concluded, based on quantum chemical calculations, that $[Li^+O^-]$ is not the active site. Calculations on cluster models illustrated that both Li/MgO and MgO possess the same nature of active sites; i.e. low coordinated MgO sites at steps and corners. This new claim thus, is that promotion with lithium does not introduce new active sites, however, enhances the concentration of defect sites in MgO. Li^+ ions and oxygen vacancies tend to segregate to the steps of MgO increasing the number of low coordinated $Mg^{2+}O^{2-}$ sites ($Mg^{2+}{}_{3C}O^{2-}{}_{3C}$), hence enhancing catalyst activity.[55,57,58,69] Consequently, improvement of catalyst selectivity, is attributed to the decrease in number of $Mg^{2+}{}_{4C}O^{2-}{}_{4C}$ sites at the steps of MgO. $Mg^{2+}{}_{4C}O^{2-}{}_{4C}$ are unselective sites and promote CO_2 formation during oxidative cracking.

The reaction model of oxidative coupling of methane on the $Mg^{2+}O^{2-}$ sites is described as follows.[57] Heterolytic bonding of CH_4 on $Mg^{2+}O^{2-}$ sites at steps and corners followed by release of methyl radicals to gas phase in presence of O_2 [Equations (9–11)].

$$[Mg^{2+}O^{2-}]_{MgO} + H{-}CH_3 \rightarrow [HO^-(Mg{-}CH_3)^+]_{MgO} \rightarrow [HO^-Mg^{\cdot -+}]_{MgO} + {}^{\cdot}CH_3 \quad (9)$$

The unpaired electron formed in this reaction facilitates O_2 chemisorption as a superoxide species:

$$[HO^-Mg^{\cdot -+}]_{MgO} + O_2 \rightarrow (O_2^-)[HO^-Mg^{2+}]_{MgO} \quad (10)$$

The reaction is very exothermic (–191 kJ mol^{-1}) and the overall process is:

$$[Mg^{2+}O^{2-}]_{MgO} + H - CH_3 + O_2 \rightarrow (O_2^-)[HO^-Mg^{2+}]_{MgO} + {}^{\cdot}CH_3 \quad (11)$$

The Mg-methylate could alternatively react with O_2 to form surface peroxo species. Despite the new hypothesis on the nature of the active sites, the reaction mechanism remains similar as proposed by Lunsford; i.e. the surface acting as a generator of radical species.

Kinetic experiments of oxidative cracking of higher alkanes; i.e. propane, *n*-butane and *n*-hexane, shows similar reaction mechanism as proposed for oxidative coupling of methane. Alkane activation takes place via the active sites of the catalyst leading to the formation of an alkyl radical [Equation (12)]. Iso-

alkyl radicals are formed more dominantly than primary alkyl radicals, due to the relative stability of the radical on the secondary carbon atom than on the primary one.[12] The later then leaves the surface and reacts further in gas phase in presence of oxygen to form cracking products [Equation (13)]. The product mixture consists of C_2–C_4 alkenes, C_1–C_5 alkanes, CO_x and H_2O.

$$C_nH_{2n+2} + O_s^- \rightarrow i{-}C_nH_{2n+1} + OH_s^- \quad (12)$$

$$C_nH_{2n+1} + O_2 \rightarrow C_1{-}C_5\ alkanes + C_2{-}C_4 olefins + CO_x + H_2O \quad (13)$$

Usually, alkane conversion increases with the increase in the carbon chain length, due to the decrease in the C–H bond strength, confirming that hydrogen abstraction from the alkane is the rate-determining step. Selectivity to alkenes change only slightly with the increase in carbon number. At 650 °C, selectivity to alkenes from cracking of ethane, propane and *n*-butane is reported to be in the range of 60–70 wt.-%.[12] Cracking products, however, change with carbon chain length depending on the decomposition routes of the primary and secondary alkyl radicals in the gas phase. For example, oxidative cracking of *n*-butane results in butene, propene and ethene, while in oxidative cracking of ethane, ethene is the only alkene observed.[12]

2.1.2 Influence of Oxygen Partial Pressures

In oxidative cracking over the Li/MgO system, oxygen plays two significant roles. Firstly, oxygen accelerates alkane conversions via the formation of hydroperoxy $HO_2\cdot$ and $OH\cdot$ radicals which act as chain propagators of the gas phase chemistry. During the oxidative cracking of both propane[12] and *n*-hexane,[14] increasing oxygen concentrations led to significant improvement in alkane conversions. Figure 1 shows the influence of oxygen partial pressures on the rate of formation of various products for the oxidative cracking of *n*-propane. Leveles et al.[12] schematically (Figure 2) described the mechanism of propane cracking, both in presence and absence of oxygen.

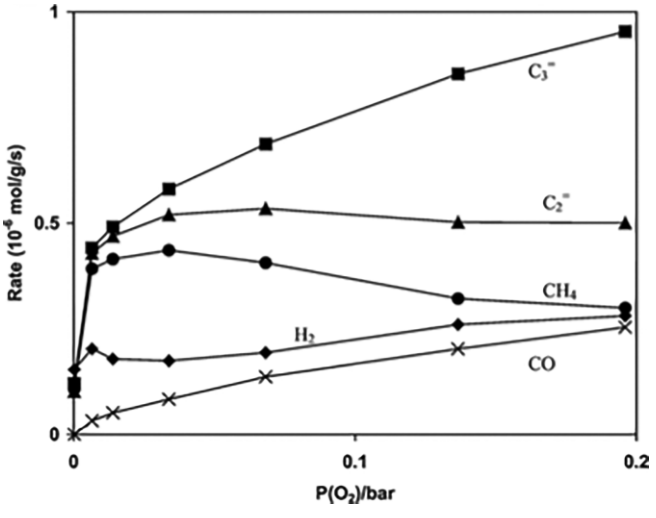

Figure 1. Rates of formation over the catalyst vs. oxygen partial pressure. Conditions: P(CO_2) = 20 mbar; P (C_3H_8) = 280 mbar; *T* = 600 °C; total flow = 100 mL min^{-1}; 200 mg of catalyst.[12]

Secondly, oxygen is necessary to regenerate the active sites of the catalyst. Two mechanisms are reported in literature.

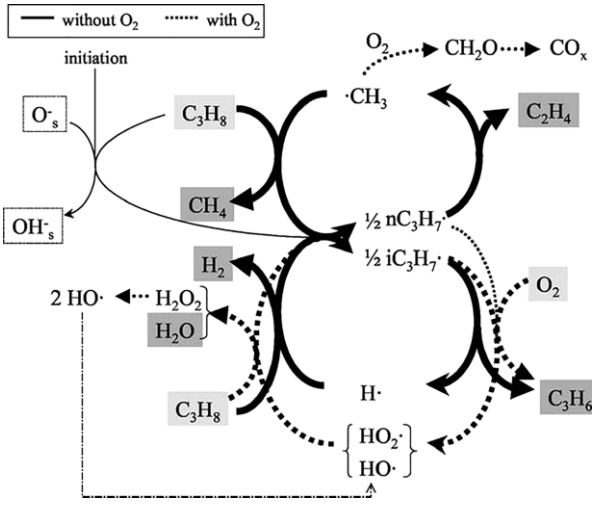

Figure 2. Reaction mechanism for the oxidative cracking of propane with and without oxygen in the feed.[12]

Equations (14–15) describe the mechanism proposed by Lunsford et al.[58] **[.]** denotes an electron trapped at an oxygen ion vacancy.

$$2Li^+OH^- \rightarrow Li^+O^- + Li^+[.] + H_2O \quad (14)$$

$$Li^+[.] + 1/2O_2 \rightarrow Li^+O^- \quad (15)$$

In oxidative cracking of propane, based on the work by Sinev and co-workers,[72–74] Leveles et al.[12] proposed a different mechanism as presented in Equations (16–19). Note that the overall regeneration reaction remains identical to the preposition made by Lunsford et al. for OCM. The critical difference is that the new mechanism does not involve the energetically very expensive removal of lattice oxygen. This is confirmed by theoretical calculations of reaction energies of surface intermediates.[74]

$$O_2 + OH_s^- \rightarrow O_s^- + HO_2 \quad (16)$$

$$HO_2 + OH_s^- \rightarrow O_s^- + H_2O_2 \quad (17)$$

$$H_2O_2 \rightarrow 2\ OH \quad (18)$$

$$OH + OH_s^- \rightarrow O_s^- + H_2O \quad (19)$$

2.1.3 Influence of Temperature

Reaction temperature has clear influence on both conversion and selectivity. Alkane conversion dramatically increases with temperature accompanied with increase in selectivity to alkenes and decrease in selectivity to CO_x.[12,14]

Figure 3 shows the influence of temperature on conversion and selectivity for oxidative cracking of propane.

At temperatures above 600 °C, gas phase activation of the alkane starts to become significant and dominates over the heterogeneous activation route via the catalyst. Therefore, in catalytic oxidative cracking, it is essential to operate at relatively low temperatures (550 to 600 °C) where gas phase initiation is negligible. However, too low temperatures, favor total combustion reactions, via the catalyst surface, minimize cracking and

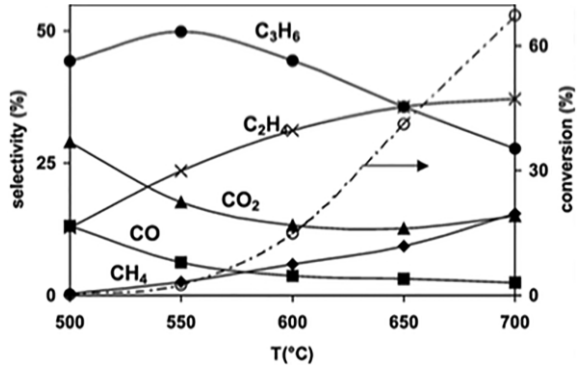

Figure 3. Conversion of propane and selectivities for various products vs. temperature over Li/MgO catalyst. Conditions: 10 % propane and 8 % oxygen in He; total flow, 10 mL min^{-1}; 100 mg of catalyst.[12]

alkene formation. At low temperatures formation of surface alkoxide species are favored from reaction of alkyl radicals with O^{2-} sites of MgO (probably on $Mg^{2+}{}_{4C}O^{2-}{}_{4C}$) [Equation (20)]. Alkoxide species are reactive and known to be intermediates in total oxidation pathways through consecutive attack by gas phase oxygen [Equation (21)].[14,75]

$$C_nH_{2n+1} + O_s^{2-} \rightarrow [OC_nH_{2n+1}^-]_s + e^- \quad (20)$$

$$[OC_nH_{2n+1}^-]_s + O_2 + e^- \rightarrow CO + CO_2 + H_2O + O_s^{2-} \quad (21)$$

2.1.4 Selectivity vs. Conversion

Interestingly and due to inherent property of Li/MgO, unlike the case with redox catalysts (V_2O_5), selectivity to alkenes remains invariant with alkane conversions.

These promising results are due to both basic and non-redox properties of the Li/MgO catalyst which prevents further adsorption and hence combustion of the product alkene. Moreover, in the oxidative cracking of propane, Leveles et al.[12] illustrated that at similar experimental conditions even in presence of gas phase oxygen, rate of conversion of propene is lower than that of propane, explaining the absence of secondary reactions of propene. Figure 4 clearly illustrates how selectivities to alkenes remain unchanged as function of propane conversion.

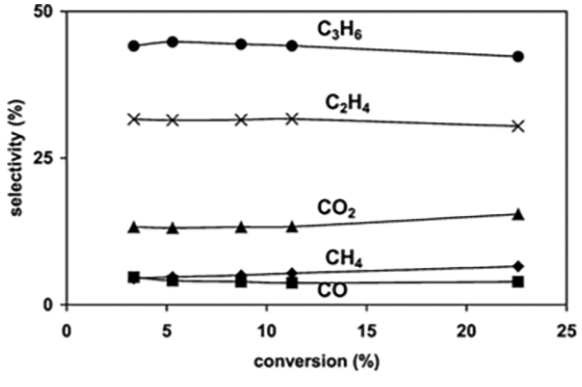

Figure 4. Selectivities for various products vs. propane conversion at 600 °C with Li/MgO catalysts. Conditions: 10 % propane and 8 % oxygen in He; total flow, 4–80 mL min^{-1}; 100 mg of catalyst.[12]

Similar observations were obtained from the oxidative cracking of *n*-hexane.[14]

2.1.5 Heterogeneous vs. Homogeneous Reaction

As mentioned above, oxidative cracking over Li/MgO is a combination of heterogeneous and homogeneous gas phase reactions. In addition to temperature, both residence time and partial pressure of the alkane have a crucial effect on gas phase initiation of cracking. To minimize extent of gas phase initiation, optimal residence times and partial pressures of the alkane are needed to minimize the extent of gas phase initiation. Leveles et al.[12] show that for oxidative cracking of propane residence times below 0.5 s are needed to limit the activation on the catalyst surface. Additionally, there is clear evidence on the effect of post catalytic free volume on enhancing gas phase reactions and hence conversions. In oxidative cracking of hexane, Boyadjian et al.,[14] similar to earlier work by Nguyen et al.,[76] reported on the effect of post catalytic volume on *n*-hexane conversions (Table 1).

Table 1. Influence of post-catalytic volume on oxidative cracking of *n*-hexane (reaction conditions: 100 mL min^{-1}, 10 % hexane, 8 % oxygen and balance He; WHSV = 15.4 h^{-1}, T = 575 °C).[14]

	Without post-cat. vol.	With post-cat. vol.
Conversion (mol-%)		
n-Hexane	28.4	33.6
Oxygen	65.2	65.5
Selectivity (mol-%)		
CO_x	24.6	20.5
CH_4	1.9	2.3
C_2–C_4 alkenes	60.7	63.3
C_2–C_4 alkanes	4.4	5.0
C_5-products	8.5	8.9

2.1.6 Promotion of Li/MgO

There is a general agreement on that promotion of Li/MgO would lead to loss of lithium, hence eventually to loss of catalytic activity.[18] Therefore promotion of Li/MgO is unfavorable and not commonly studied. Basically, three types of promoters have been studied: (1) promotion with a rare earth metal; e.g. Dy,[18,20] (2) promotion with a halogen[18,19] and promotion with redox promoters such as Mo, V and Bi,[14] discussed in section 2.1.7.

In Li/Dy/MgO, addition of Dy_2O_3 to Li/MgO, decreases catalyst activity by a factor of two, together with slight decrease in selectivity. Thus, the additional Dy_2O_3 system results in an negative effect on catalyst performance, due to the loss of lithium as $LiDyO_2$.[18]

Chlorine-containing Li/MgO exhibits high activity and selectivity to alkenes in oxidative cracking reactions; however, the catalyst suffers from deactivation due to loss of Cl. Lercher and co-workers[18,19] investigated the role of chlorine addition on performance of Li/Dy/MgO for the oxidative cracking reactions. Figure 5 illustrates these results. Chlorine-containing catalyst shows clear deactivation; thus, researchers conclude that Li is the only essential addition to magnesia.

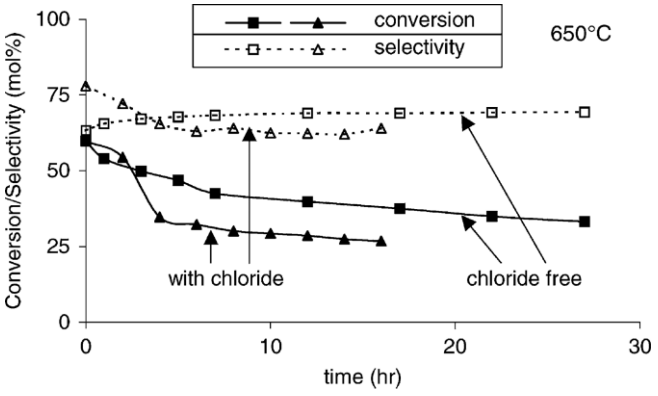

Figure 5. Effect of chloride addition on the conversion (filled symbols) and selectivity (open symbols) of the Mg-Dy-Li-Cl (triangle symbols) and Mg-Dy-Li (square symbols) catalysts with time on stream. Feed, propane; WHSV, 1 h^{-1}.[18]

2.1.7 Stability of Li/MgO

One drawback of the Li/MgO system is the loss of activity with time, especially within the first hours of reaction. Different deactivation mechanisms are reported depending on the nature of the active sites considered. With the claim of the $[Li^+O^-]$ sites as the active sites of the catalyst, the role of product CO_2 in poisoning of these sites was reported repeatedly.[12,14,15] The product CO_2 inhibits reaction by adsorption on the $[Li^+O^-]$ sites of the catalyst forming Li_2CO_3, the presence of which has been detected by TPD of carbon dioxide.

With the recent claim however, considering the low coordinated $Mg^{2+}{}_{LC}O^{2-}{}_{LC}$ sites at the steps and corners of MgO as the active sites of the catalyst, catalyst deactivation is attributed to sintering enhanced by presence of Li_2CO_3. In MgO, sintering leads to drastic changes in the primary particle morphology as indicated by electron microscopy and spectroscopic techniques, which in turn leads to loss of defect sites (active sites) on the steps and terraces of MgO.[56,67]

Doping the catalyst with redox promoters like molybdenum and bismuth helps to maintain catalyst stability, hence achieve higher yields of light alkenes.[15] It is believed that the presence of the dopant repels CO_2 and significantly inhibits Li_2CO_3 formation, hence preventing sintering and preserving catalyst activity. Low concentrations of the dopant are sufficient to improve catalyst stability. Higher concentrations lead to combustion via Mars-van-Krevelen oxidation/reduction cycles, moreover as mentioned in the earlier section, high concentrations of dopants would lead to loss of lithium and are hence unfavorable.[37] Figure 6 shows TPD of CO_2 from doped and undoped Li/MgO catalyst after being used for the oxidative cracking of *n*-hexane. Doped catalyst results in significantly lower CO_2 desorption peak.

In addition to sintering, in oxidative coupling of methane at high reaction temperatures, there is evidence of lithium loss via volatilization. This is however less relevant for oxidative cracking because of the milder reaction temperatures used.[67]

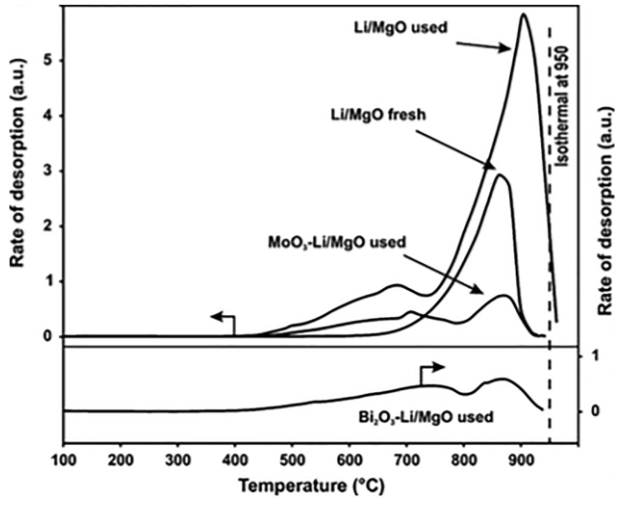

Figure 6. Temperature programmed desorption of CO_2 for fresh and used catalysts (TPD in situ after catalytic reaction, signals are normalized to the BET surface area). Temperature ramp 10 °C min^{-1}, He 10 mL min^{-1}.[14]

2.2. Rare Earth Oxides

Various rare earth oxides have been studied in literature for the oxidative cracking of *n*-butane, these include: (1) stoichiometric rare earth oxides such as La_2O_3, Sm_2O_3, Eu_2O_3, Gd_2O_3 and (2) non-stoichiometric rare earth oxides such as CeO_2, Pr_6O_{11} and Tb_4O_7.[8] Oxidative cracking over non-stoichiometric rare earth oxides proceeds via redox reaction involving lattice oxygen. This results in low catalyst activity and selectivity to alkenes as result of total oxidation and significant CO_x formation.

Amongst various rare earth oxides tested, Sm_2O_3 shows highest activity and selectivity to C_2–C_4 alkenes. At 600 °C ca. 37 and 25 wt.-% yield to alkenes and CO_x is reported, respectively. Oxidative cracking over rare earth oxides proceeds via hydrogen abstraction from the alkane by active surface oxygen species, O^{2-} and O^-, forming alkyl radicals which undergo β-scission and further crack in gas phase.[22–24] CO_2 formation over these catalyst systems results from interaction between intermediate radicals/alkenes and active oxygen species. This is favored at low temperatures due to the long-life adsorbed radicals. Nevertheless, at high temperatures the rate of the release of these intermediate species is increased leading to lower CO_x formation.

Promotion of rare earth oxides with alkali metals results in further improvement in catalyst performance. Figure 7 shows that, for oxidative cracking of *n*-butane, doping of La_2O_3 with Na, Li and K results in significant improvement in selectivities to light alkenes,[8] the extent of which would depend on the type of the alkali metal. It is commonly observed that of all alkali metals, Li doping results in best selectivities to alkenes. For oxidative cracking of *n*-butane at 700 °C, Li/La_2O_3 results in 79 wt.-% selectivity to alkenes. The catalyst however exhibits relatively low activity for *n*-butane conversion (19 wt.-% *n*-butane conversion).[24] Amongst various Li doped rare earth oxides (Li/La_2O_3, Li/Sm_2O_3, Li/Gd_2O_3, Li/Y_2O_3), Li/Y_2O_3 exhibits best activity and yields of alkenes. Oxidative cracking of *n*-butane over Li/Y_2O_3 at 700° results in 39 wt.-% yield of C_2–C_4 alkenes.[24] In general the positive effect of alkali metal doping is associated to the role of the latter in weakening the adsorption of intermediate hydrocarbon species as well as alkenes to

the catalyst surface. Apparently, this effect strongly depends on the type of the alkali metal. In case of Li/Y_2O_3, the presence of a thin layer of Li_2CO_3 is reported, which enhances the formation of new active oxygen species, in addition to hindering deep oxidation reactions.[24]

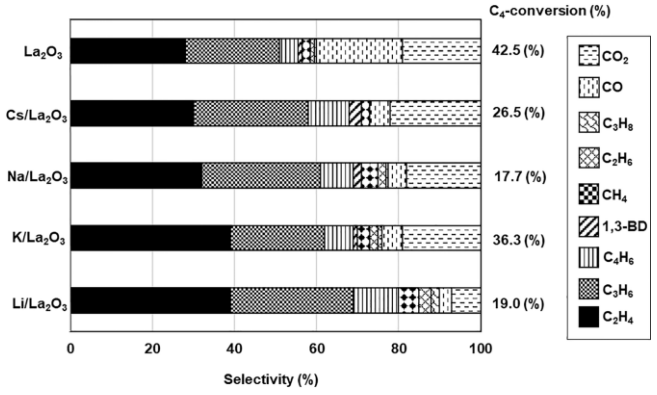

Figure 7. Changes in selectivity after modifying La_2O_3 with alkali metals. Reaction temperature = 600 °C; W/F = 0.43 g s/mL; feed *n*-butane/oxygen/nitrogen/helium = 1.4/1.5/5.6/88.5 (mL min^{-1}, NTP); molar ratio of alkali metal/La = 1.0.[8]

More recently, Sa et al.[26] reported on the oxidative cracking of *n*-butane over Au/La_2O_3. At 650 °C, ca. 40 wt.-% conversion and 47.7 wt.-% selectivity to alkenes is achieved. The active site is believed to be a combination between cationic gold and lanthanum oxide, which activates the *n*-butane at low temperatures. The catalyst is selective towards alkene formation and does not provide sites for combustion reactions, leading to low CO_x formation. The addition of gold also appears to stabilize lanthanum oxycarbonate species that may play a role in enhancing the performance of the gold-promoted oxides catalysts.

2.3. Oxychlorides

Oxychlorides show good performance and relatively good stability for oxidative cracking reactions. Yoshimura and co-workers[33] reported on the oxidative cracking of *n*-butane over oxychlorides such as BiOCl, LaOCl, and SmOCl. Compared to LaOCl and SmOCl catalysts, BiOCl catalyst shows selectivity for higher alkenes and suppresses deep oxidation reactions. At 600 °C, BiOCl, results in 50.7 wt.-% conversion of *n*-butane and 73.4 and 25.6 wt.-% selectivity to total alkenes and CO_x, respectively. SmOCl, results only in 27.4 wt.-% conversion of *n*-butane with 46.8 wt.-% selectivity to light alkenes and 52.5 wt.-% selectivity to CO_x. Thus, deep oxidation reactions are favored over both lanthanum and samarium-containing catalysts.

The difference of catalytic performances among *A*OCl (*A* = Bi, La, Sm) catalysts is ascribed to the difference in active centers on the surface of these catalysts. Generally, it is considered that lanthanum and samarium ions in the oxychloride catalysts can form activated oxygen species for deep oxidation of *n*-butane.[8,20] However, the nature of active centers on the oxychloride catalysts is not well understood yet.

The cracking severity on BiOCl increases with temperature. At the higher temperature (ca. 600 °C) selectivity to ethene increases, while at lower temperatures (500 °C) dehydrogenation reactions are favored resulting in butene, butadiene and propene. Similar to Li/MgO, it has been proposed that oxidative cracking of *n*-butane over BiOCl is initiated by hydrogen abstraction and butyl radical formation. At high reaction temperatures, the butyl radical is cracked to give ethene and ethyl radical or propene and methyl radical due to β-scission. At lower temperatures, the butyl radical is mainly dehydrogenated to produce butene. Water is formed from oxidation of abstracted hydrogen by gas phase oxygen.

BiOCl catalyst is considered relatively stable under reaction conditions for oxidative cracking of *n*-butane. Only at temperatures above 650 °C, the formation of a new $Bi_{24}O_{10}Cl_{31}$ phase is observed, which is considered to be inactive and selective for the oxidative cracking reactions. Thus at temperatures above 650 °C, the performance of the catalyst deteriorates.

2.4. Boria-Containing Catalysts

One of the earliest papers that appeared on oxidative conversion of propane was in 1998. Buyevskaya et al.[30–32] reported on the oxidative conversion of propane over boria-containing Al_2O_3, TiO_2, ZrO_2 and MgO catalysts. Boria supported on alumina, shows best performance with the highest yields to alkenes.

The catalyst shows in addition to dehydrogenation and partial oxidation, cracking activity; thus leads to the formation of cracking products such as ethene and methane. The performance of the catalyst depends very much on the catalyst preparation method. For the oxidative conversion of propane at 550 °C, B_2O_3/Al_2O_3 prepared from aqueous solution of boric acid and alumina results in highest cracking activity (42 wt.-% propane conversion) with 26.5 % yields to propene and ethene, and only 10.1 wt.-% and < 1.7 wt.-% yields to CO_x and C_1–C_2 oxygenates, respectively. Catalyst prepared by wetness impregnation results in 30 wt.-% conversion of propane, with 16.5 wt.-% yields to propene and ethene, and 4 wt.-% and 8 wt.-% yields to CO_x and C_1–C_2 oxygenates, respectively.

Structure-performance study using XRD characterization shows the formation of different crystalline and amorphous boron-containing phases depending on the preparation method. It is shown the trigonal BO_3 species, present in both amorphous and crystalline phases, are responsible for catalytic activity. Catalyst prepared from aqueous solution of boric acid and alumina contains amorphous BO_3 phase. This, however, is found to be unstable and volatile under reaction conditions through reaction with product water and formation of boric acid. Catalyst prepared by wetness impregnation contains crystalline B_2O_3, $Al_4B_2O_9$ and $Al_6B_8O_{21}$ phases. The catalyst is relatively more stable than one prepared from aqueous solution however, again in this catalyst loss of boron through reaction with water remains unavoidable. $Al_4B_2O_9$ is found to be not active for propane conversion and $Al_6B_8O_{21}$ phase active for formation of oxygenates.

The activity for propane conversion of B_2O_3/Al_2O_3 catalyst is attributed to the Lewis acidity of the catalyst.[32] It is suggested,

that Lewis acid sites generate propyl radicals which further react in gas phase forming cracking products and oxygenates. However, increase in propane conversions results in significant decrease in selectivities to propene (dehydrogenation product) and significant increase in CO accompanied with gradual increase in selectivity to ethene (cracking product) and CO_2. Figure 8 shows the effect of propane conversion on selectivities to various products. The observed product dependency on conversion suggests that partial oxidation becomes significant at high conversions, leading to enhanced thermal cracking and hence enhanced ethene formation.

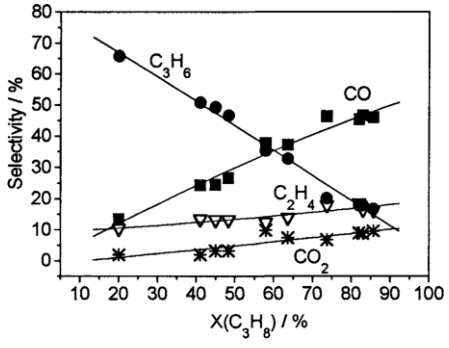

Figure 8. The dependence of product selectivities on propane conversion on B_2O_3 (30 wt.-%)/$A1_2O_3$; T = 550 °C, $p(C_3H_8)$ = 25 kPa, $p(O_2)$ = 50 kPa.[30]

2.5. Gold-Containing Catalysts

Gold supported on sulfated CeO_2-ZrO_2 (Au-SCZ) is reported as a promising catalyst for the oxidative cracking of propane. Narasimharao et al.[27] presents a comparative study of oxidative cracking of propane over both sulfated and unsulfated gold supported on ceria-zirconia catalysts. Figure 9 illustrates the performance of these two catalysts as function of temperature. Au-SCZ exhibits superior performance over the unsulfated catalyst. The catalyst shows cracking activity at temperatures as low as 400 °C. At this temperature ca. 28 wt.-% conversion of propane is achieved with ca. 88 wt.-% selectivity to light alkenes (ethene, propene and butene). At 650 °C, ca. 62 wt.-% conversion of propane is achieved with ca. 68 wt.-% selectivity to light alkenes (ethene, propene and butene). The catalyst is stable over 48 h of reaction and no carbon deposition is observed.

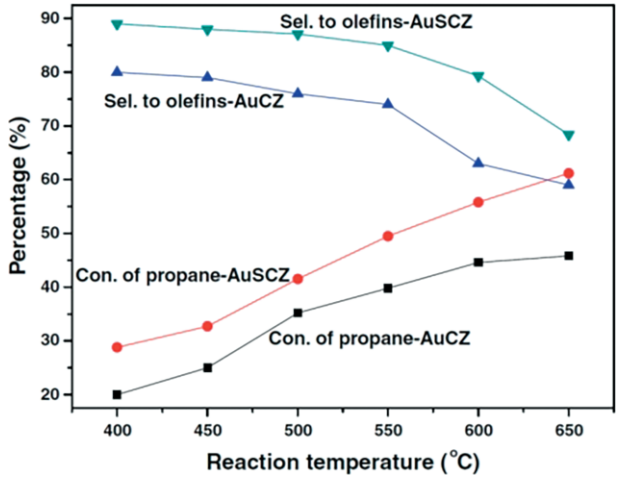

Figure 9. Conversion of propane and selectivity to alkenes over AuCZ and AuSCZ samples.[27]

The high activity of Au-SCZ is explained by the role of sulfation in improving dispersion of gold particles, in increasing the amount and strength of acid sites and in formation of easily reducible interactive species between the gold particles and the $Ce_{0.5}Zr_{0.5}O_2$ surface. This conclusion is based on observations from characterization experiments. TEM images of Au-SCZ (Figure 10) show homogeneous dispersion of lower size nanoparticles and DRIFT pyridine adsorption tests reveal that sulfation increases the strength of the Lewis sites and creates new Brønsted sites.[80] Considering the acidic nature of the surface, the authors propose that reaction proceeds via protonation of propane on the catalyst surface forming $C_3H_9^+$ which decomposes into H_2 and $C_3H_7^+$ or CH_4 and $C_2H_5^+$. Propene and ethene are formed after deprotonation of $C_3H_7^+$ and $C_2H_5^+$, respectively.

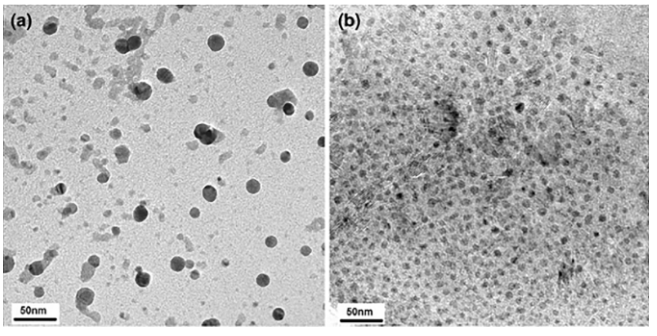

Figure 10. TEM images of (a) AuCZ and (b) AuSCZ.[27]

2.6. Nitrogen-Containing Co-Al_2O_3

In addition to Au-SCZ, nitrogen-containing Co-Al_2O_3 is identified as a promising catalyst for low temperature (400 °C) cracking of propane.[28,29] The catalyst is prepared by deposition of cobalt and nitrogen-containing precursor [sodium salt of (4,5-carboxy)-cobaltphthalocyanine] on ϒ-Al_2O_3 followed by thermal decomposition in stream of He at 700 °C.

Nitrogen doping improves the performance of Co-Al_2O_3 catalyst. The low temperature cracking activity is a special characteristic of this catalyst. 0.8Co-N exhibited best performance. At 400 °C, ca. 25 wt.-% yield of light alkenes is observed with *n*-butane cracking and 14 wt.-% yield of alkenes with propane. These are higher than yields obtained on any other system studied so far for the oxidative conversion of propane and *n*-butane (Figure 11). Temperature increase from 400 to 600 °C results in increase in alkene yields. At 600 °C, 47.6 and 37.4 wt.-% yield of light alkenes is observed at 82 and 76.6 wt.-% *n*-butane and propane conversions, respectively.

Catalyst characterization by SEM, X-ray photoelectron spectroscopy (XPS), XRD and TPR studies suggests that a stable cobalt oxynitride phase is formed. This resulted in lowering the oxygen binding energy leading to enrichment in mobile, low

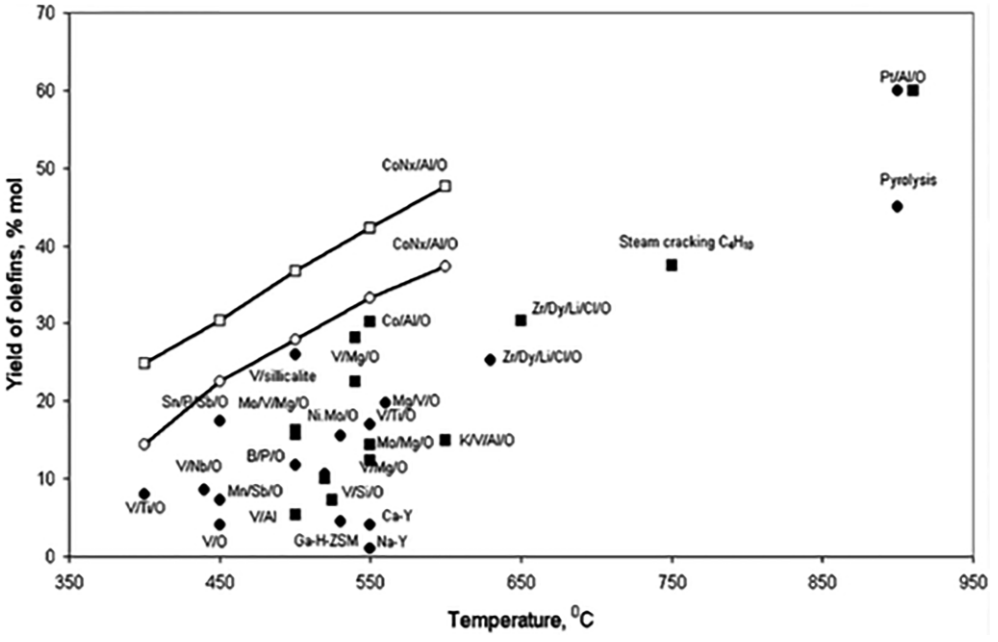

Figure 11. Comparison of performance of various catalyst systems for the oxidative cracking of propane (circles) and *n*-butane (diamond).[28]

energy, oxygen species that significantly accelerates cracking activity and hence alkene formation.

2.7. Non-Conventional Reactor Systems

The catalysts discussed so far have been tested in packed bed reactors. In this section we will discuss other types of reactors.

2.7.1 Pt Coated Monoliths

In the nineties, Schmidt and co-workers[46–54] reported on the oxidative conversion (dehydrogenation and cracking) of alkanes into alkenes over Pt-coated monoliths at short contact times of milliseconds. The oxidative conversion of lower alkanes (ethane, propane, butane)[46–50] and higher alkanes (pentane, isopentane, *n*-hexane, n-decane)[53,54] was investigated on various noble metal catalysts such as Pt, Rh and Pd at different alkane/oxygen ratios in adiabatic tubular reactors (autothermal operation). The reaction mixture was preheated to between 200–250 °C and then heated to temperature > 900 °C by the exothermic oxidation reactions.

Both type of noble metal and alkane-to-oxygen ratio have clear influence on the product distribution. On Pt, for example, synthesis gas and alkene formation is observed at stoichiometry and high alkane-to-oxygen ratios, respectively, with no carbon deposition and catalyst deactivation. Rh favors the formation of synthesis gas (CO and H_2) while on Pd carbon deposition deactivates the catalyst.

Dehydrogenation reactions are favored over cracking at high alkane-to-oxygen ratios over a Pt-coated alpha-Al_2O_3 foam monolith. At these conditions, oxidative conversion of propane and butane results in the formation of light alkenes such as ethene, propene and butene. High temperatures favor formation of ethene while low temperature and short contact times favor formation of propene. At conversions of propane and *n*-butane higher than 90 wt.-%, 55–60 and 65–70 wt.-% selectivity to light alkenes is observed, respectively. At high alkane-to-oxygen ratios, the oxidative conversion of higher alkanes, such as *n*-pentane and *n*-hexane results in formation of C_5 and C_6 linear alkenes, respectively.

Schmidt and co-workers proposed that for dehydrogenation, surface reactions are dominant over homogeneous reactions. Similar to the mechanism over Li/MgO, the catalyst surface initiates alkane dissociation by hydrogen abstraction by adsorbed oxygen on Pt (oxidative dehydrogenation) leading to a surface alkyl. β-hydrogen and β-alkyl elimination reactions of the adsorbed alkyl lead to dehydrogenation and some cracking.

At low alkane-to-oxygen ratio (oxygen rich environment) however, cracking reactions dominate over dehydrogenation. At these conditions, oxidative conversion of *n*-pentane and *n*-hexane form primarily ethene and propene. The product distribution is quite similar to that of thermal pyrolysis of the same alkanes. Hence, it is proposed the presence of two consecutive reactions: (1) surface initiated partial oxidation to CO, CO_2 and H_2O by oxygen atoms adsorbed on platinum, followed by (2) thermal cracking in gas phase.

In oxidative cracking of *n*-decane and *n*-hexadecane, similar trends are observed. Increasing C/O ratio shifts the product from syngas to light alkenes then to α-alkenes. In general, observations made by Schmidt and co-workers[46–54] in partial oxidation of alkanes over Pt-alumina catalysts at millisecond contact times suggest that for the lower alkanes, relatively low temperatures, short contact times and high alkane-to-oxygen ratios favor surface dehydrogenation reactions. Higher alkanes and low alkane-to-oxygen ratios favor oxidation and cracking reactions.

2.7.2 Integrated Plasma-Catalyst Systems

Integrated plasma-catalyst systems have been reported in literature for the decomposition of hydrocarbons. Boyadjian et

al.[44,45] reported on the oxidative cracking of *n*-hexane with Li/MgO in presence of DBD non-equilibrium plasma at temperatures between 500 and 600 °C. Plasma catalytic cracking results in considerable improvements in the yields of light alkenes indicating the presence of synergy. At 600 °C, integrated plasma-Li/MgO system results in 34 % yields of C_2–C_4 alkenes, while the catalyst system alone results in 18 % yields of alkenes.

Presence of plasma provides new routes for C–C and C–H bond dissociation via electron impact excitation of the alkane. The following hexane dissociation routes were proposed: (1) C–C, C–H bond scission by electron-impact excitation of hexane molecules [Equations (22–25)] and (2) C–H bond scission by collision of hexane molecules with $O(^3P)$ oxygen atoms [Equation (26)] formed from electron impact excitations of molecular oxygen [Equations (27–28)].

Reaction of molecular oxygen with hexyl radicals form HOO· radicals [Equation (29)] which act as the main chain propagators and increase the radical concentration during oxidative conversion.

$$C_6H_{14} + e^- \rightarrow C_6H_{13} + H\cdot + e^- \quad (22)$$

$$C_6H_{14} + e^- \rightarrow C_5H_{11} + CH_3 + e^- \quad (23)$$

$$C_6H_{14} + e^- \rightarrow C_4H_9 + C_2H_5 + e^- \quad (24)$$

$$C_6H_{14} + e^- \rightarrow C_3H_7 + C_3H_7 + e^- \quad (25)$$

$$C_6H_{14} + O(^3P) \rightarrow C_6H_{13} + OH\cdot \quad (26)$$

$$O_2 + e^- \rightarrow 2O(^3P) + e^- \quad (27)$$

$$O_2 + e^- \rightarrow O(^3P) + O(^1D) + e^- \quad (28)$$

$$O_2 + C_6H_{13} \rightarrow C_6H_{12} + HOO\cdot \quad (29)$$

Moreover, presence of plasma helps generating new active sites on the catalyst. It is reported that UV light generated by plasma, leads to the ionization of low-coordinated surface oxygen anions $(O^2)^-$ LC in MgO, forming a localized surface hole state [O^-] and a surface-trapped electron [Equation (30)].[77]

$$O^{2-}_{LC} + h\nu \rightarrow O^-_{LC} + e^- \quad (30)$$

These [O^-] defect sites created by the plasma, similar to the [Li^+O] sites, could also enhance H· abstraction from the alkane forming alkyl radical.

Generally, in plasma-catalysis it is believed that radicals generated by plasma would further interact with the catalyst surface. Experiments on varying plasma-catalyst positions in the reactor clearly illustrate that further interaction of the radicals with catalyst surface is resulting in dehydrogenation, alkene formation as well as combustion.[41–45] This, however, is very complex because plasma contains many other species, e.g. ions, electronically as well as vibrationally excited species. Furthermore, the properties of the plasma are influenced by the presence of the catalyst, and vice versa, the catalyst is influenced by the plasma. The complexity of this is enormous and insight is still very limited.[78,79]

2.8. Comparative Summary of Various Catalyst Systems

Table 2 presents a summary of the performance of all catalyst systems mentioned in this review for the oxidative cracking of *n*-propane and *n*-butane in temperature ranges between 400 and 900 °C. Both Au-SCZ and Co-N/Al_2O_3 are especially important catalysts showing cracking activity at low temperatures (400 °C) while no other catalyst system exhibits cracking activity at low temperatures as such. At temperatures between 550–650 °C Li/Cl/Dy/MgO results in highest yields to alkenes, however, it is unstable and its use is not very much favored. For this temperature range, amongst Au-SCZ, Co-N/Al_2O_3 and Li/MgO catalysts, Au-SCZ is the most selective catalyst resulting in highest yields to alkenes thus, the most promising.

The application of Li/MgO stays somehow limited due to considerable formation of CO_2. Deactivation of Li/MgO catalysts occurs as result of Li_2CO_3 formation and sintering. Catalyst stability is improved via addition of traces of molybdenum or bismuth metals, which play a significant role in inhibiting formation of Li_2CO_3 thus preventing sintering and loss of activity. Plasma-Li/MgO system is found to be very promising for the formation of high yields of alkenes due to the synergy effect created. Despite the ability of plasma to generate radicals at room temperature, cracking still requires high temperatures. At room temperature alkyl radicals formed in plasma tend to couple and form higher alkanes.

Au/La_2O_3 exhibits an average performance, which makes it less attractive as compared to above mentioned catalyst systems. The application of BiOCl for oxidative cracking is limited

Table 2. Conversions and selectivities from oxidative cracking of *n*-propane and *n*-butane over various catalyst systems (for Li/Y_2O_3, BiOCl and Au/La_2O_3 only data of *n*-butane cracking is available in literature).

Catalyst	Reaction conditions	Conv. (%)	Sel. to alkenes (%)	Yield of alkenes (%)	Ref.
Li/MgO	C_3H_8/O_2/He = 10/8/82, *T* = 650 °C, WHSV = 0.8 h^{-1}	64.0	55.9	35.8	[12]
Li/Cl/Dy/MgO	C_3H_8/O_2/He = 10/8/82, *T* = 650 °C, WHSV = 0.8 h^{-1}	76.0	69.0	52.4	[18]
Plasma-Li/MgO	C_6H_{14}/O_2/He = 10/8/82, *T* = 600 °C, WHSV = 3.08 h^{-1}	55.0	64.0	35.2	[45]
Au/SO_4^{2-}/$Ce_{0.5}Zr_{0.5}O_2$	C_3H_8/O_2/air = 20/10/70, *T* = 400 °C, WHSV = 36 h^{-1}	28.0	88.0	24.6	[27]
Au/SO_4^{2-}/$Ce_{0.5}Zr_{0.5}O_2$	C_3H_8/O_2/air = 20/10/70, *T* = 650 °C, WHSV = 36 h^{-1}	62.0	68.0	42.2	[27]
CoN_x/Al_2O_3	C_3H_8/O_2 = 1/1.5, *T* = 400 °C, WHSV = 5 h^{-1}	24.0	59.0	14.2	[28]
CoN_x/Al_2O_3	C_3H_8/O_2 = 1/1.5, *T* = 600 °C, WHSV = 5 h^{-1}	77.0	49.0	37.7	[28]
B_2O_3/Al_2O_3[a]	C_3H_8/O_2 = 25/50, *T* = 550 °C, *x* = 2 g s mL^{-1}	20.0	75.0	15.0	[30]
Pt/Al_2O_3	C_3H_8/O_2/He = 17.5/17.5/65, *T* = 900 °C, 5 SPLM	74.0	58.0	42.9	[46]
Li/Y_2O_3	*n*-C_4H_{10}/O_2/He = 8/8/84, *T* = 700 °C, 180 mL min^{-1}	51.0	77.0	39.3	[24]
Au/La_2O_3	*n*-C_4H_{10}/O_2/He = 1.1/0.6/98.3, *T* = 650 °C, 220 mL min^{-1}	40.0	47.7	19.1	[26]
BiOCl	*n*-C_4H_{10}/O_2/He = 1.1/0.6/98.3, *T* = 650 °C, 220 mL min^{-1}	20.0	21.1	4.2	[26]

[a] Catalyst prepared by wet impregnation.

to a very narrow temperature window between 600 and 625 °C; above this temperature an inactive and unselective phase is formed on the catalyst. B_2O_3/Al_2O_3 exhibits very high selectivity to alkenes at 550 °C, however selectivity on this catalyst is conversion dependent and would decrease at high conversions due to oxidation of intermediate alkyl species. The performance of Li/Y_2O_3 is only reported at temperatures above 700 °C, therefore it is difficult to draw conclusions on the suitability of this catalyst due to lack of experimental data. Partial oxidation over Pt/Al_2O_3 monoliths at short contact times is a high temperature application, hence would not bring the advantage of low temperature cracking.

3. Technical and Economic Evaluation

The potential industrial application of the catalytic oxidative cracking (COC) process depends on both the technical and economic advantages the process is able to achieve, as compared to the conventional steam cracking process. Thus, to evaluate the oxidative cracking process, a comparative study of both processes is essential.

At the University of Twente, we performed a process design of the oxidative cracking process, utilizing experimental data from the cracking of *n*-hexane.[16] Figure 12 presents a functional block diagram of the two processes, highlighting the key differences. The key process differences between the two processes are the following:

(1)COC uses catalyst and hence a catalytic reactor. A catalytic reactor would require smaller investment costs compared to the steam cracking furnaces.

(2)COC uses oxygen in the feed with no diluent while SC uses steam as diluent. Two feeding options are possible:

• Pure oxygen as the feed: Need for air separating unit and necessity to ensure safe operation outside the explosion limits.

• Air as the feed: Need for N_2 separation unit to separate N_2 from the products.

(3) Steam cracking operates at 800 °C while COC operates at 550–600 °C. Steam cracking uses an external source of heating where methane is used as fuel, while in oxidative cracking part of the heat of reaction is provided auto-thermally inside the reactor, hence reducing external fuel combustion. Consequently, oxidative cracking consumes less energy than steam cracking process.

(4) Different product distribution and ratio of C_3–C_4 alkene/ethene. Table 3 presents data of naphtha cracking from oxidative cracking experiments performed with the support of BASF in Ludwigshafen compared to that of steam cracking. Oxidative cracking results in CO_2 production and higher ratio of C_3–C_4 alkenes-to-ethene. This leads to different separation trains, es-

Table 3. Comparison of product distribution from catalytic oxidative cracking (COC) and steam cracking of naphtha.

	Naphtha COC	Naphtha steam cracking
Conversion (wt.-%)		
Naphtha	50.0	85.0
Oxygen	93.0	
Selectivity (wt.-%)		
C_1–C_4 alkanes	14.3	18.0
Ethene	21.5	27.2
Propene	22.1	17.3
C_4-alkenes	12.4	6.1
Butadiene	3.8	4.7
> C_5-products	16.7	25.1
CO	5.7	0.1
CO_2	3.1	0.0
H_2	0.4	0.9
$(C_3^= + C_4^=)/C_2^=$	1.6	0.9
Product value (Euro/t)	130.0	170.0

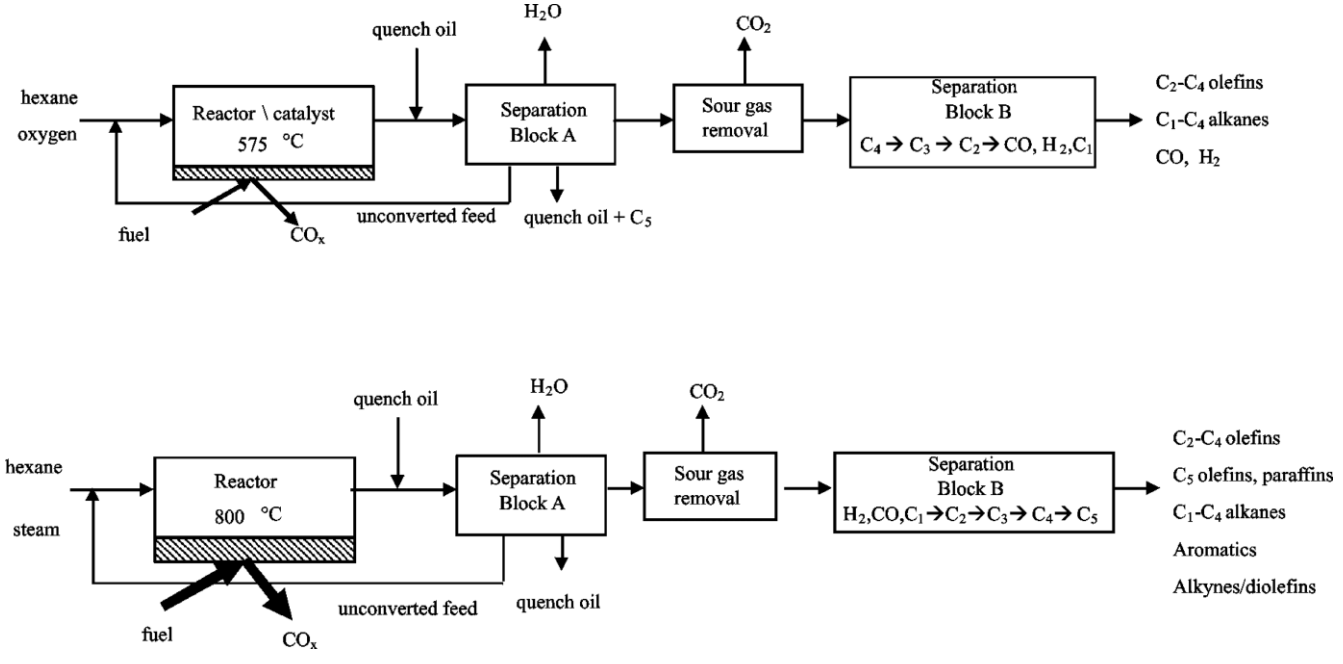

Figure 12. Key process differences between the COC and SC processes.[16]

pecially in block B (Figure 12). Steam cracking process is designed for a maximum ethene production and recovery; hence, light alkenes are separated first. Oxidative cracking process is designed for production and recovery of propene and butene; hence, these alkenes are separated first. The separation of heavy products and quench oil (block A in Figure 12) in both processes is similar.

An economic evaluation of the oxidative cracking process, presented by J.-P. Lange from Shell Laboratories, shows that the potential savings in the investment costs of the COC process, as result of the use of smaller catalytic reactor, are significantly offset by the cost of oxygen purification plant.[17]

Additionally, our results indicate that 74 % of the operational costs of the COC process are costs of naphtha feed. This implies that carbon loss as a result of combustion of part of the valuable naphtha feed makes the COC process economically less attractive than steam cracking. Moreover, the heat utilities present only 3 % of the total operational costs, which implies that the energy efficiency of the COC process as compared to SC does not result in significant savings in operational costs.

The product value of the COC process, due to the presence of CO_2, stays below that of steam cracking (Table 3). Using current market prices of naphtha, ethene, propene and butene, COC results only in marginal revenues over the operational costs. These strongly suggest that the COC process is not economically feasible yet. The economic feasibility of oxidative cracking would depend on developing a process which would bring yields of alkenes to comparable values as in steam cracking. This would necessitate the development of efficient combination of catalyst-reactor systems. Moreover, since oxidative cracking process results in formation of more of C_3–C_4 alkenes than ethene, any increase in market prices of C_3–C_4 alkenes would potentially improve the overall product value of the process.

4. Reactor Design

Reactor design and research work investigating the development of optimized reactor-catalyst systems would be essential in further improving yields of alkenes for oxidative cracking reactions. Fluidized bed and membrane reactors are conceptually potential reactors for the oxidative cracking reactions. These reactors allow for staged oxygen admission to the reactor, hence maintaining low oxygen partial pressures in the reactor and reducing extent of combustion reactions. For the oxidative dehydrogenation of ethane, for example, the use of a multitubular membrane reactor results in significant improvements in the yields of ethene.[81] For the same application, another research group has investigated the use of fluidized bed membrane reactor.[82] For oxidative cracking similar reactor design could be considered with ensuring the presence of void spaces for enhancement of homogeneous alkyl radical reactions.

5. Conclusion

We presented a review on the catalytic oxidative cracking of lower alkanes with focus on the Li/MgO system. Oxidative cracking is initiated on the catalyst surface followed by thermal cracking in the gas phase. The potential catalyst should possess active and selective sites for hydrocarbon activation and alkene formation, and minimize extent of total oxidation reactions. A comparative study of Li/MgO with various catalyst systems reported in literature shows that the application of Li/MgO stays somehow limited due to considerable formation of CO_2. Recent literature work on both Au-SCZ and Co-N/Al_2O_3 shows the significance of these catalyst systems for oxidative cracking at temperatures as low as 400 °C. Au-SCZ exhibits superior selectivity to alkenes with very low activity for combustion reactions, which makes it a promising catalyst for further study.

Combined catalyst-plasma systems result in synergy effect and enhanced alkene yields. The chemistry of these systems is very complex and not yet fully understood. Very high yields of alkenes are also achieved with oxidative cracking at short contact times over Pt/Al_2O_3 monoliths. However, this is considered a high temperature application and would therefore not bring the advantage of low temperature cracking.

Despite of the relatively high yields of alkenes achieved with the best catalysts mentioned in this review (e.g. Au-SCZ), CO_2 formation is inevitable and introduces challenges in the technical and economic feasibility of the process and its attractiveness over the state-of-art steam cracking. Future work should focus on reactor design and the development of optimized reactor-catalyst systems aiming towards commercially acceptable yields of alkenes in oxidative cracking reactions. The reactor system should allow for staged oxygen admission and ensure the presence of void spaces for enhanced gas phase propagation of intermediate radicals. Gas phase reactions would lead to alkene formation and partial oxidation rather than CO_2 which is characteristic of surface-promoted total oxidation reactions. The combination of optimal reactor design and selective catalyst system is the key for achieving commercially acceptable yields of alkenes.

Keywords: Cracking · Oxidation · Alkanes · Alkenes · Li/MgO · Au-SCZ

[1] H. Zimmermann, R. Walzl, *Ullmann's Encyclopedia of Industrial Chemistry*, Wiley-VCH, Weinheim, **2009**.
[2] BP Statistical Review of World Energy, BP Technical Report, London, **2013**.
[3] P. C. Bruijnincx, B. M. Weckhuysen, *Angew. Chem. Int. Ed.* **2013**, *52*, 11980–11987; *Angew. Chem.* **2013**, *125*, 12198.
[4] J. J. Siirola, *AIChE J.* **2014**, *60*, 810–819.
[5] I. Amghizar, L. A. Vandewalle, K. M. Van Geem, G. B. Marin, *Engineering* **2017**, *3*, 171–178.
[6] T. Ren, M. Patel, K. Blok, *Energy* **2006**, *31*, 425–451.
[7] V. S. Arutyunov, R. N. Magomedov, A. Yu. Proshina, L. N. Strekova, *Chem. Eng. J.* **2014**, *238*, 9–16.
[8] Y. Yoshimura, N. Kijima, T. Hayakawa, K. Murata, K. Suzuki, F. Mizukami, K. Matano, T. Konishi, T. Oikawa, M. Saito, T. Shiojima, K. Shiozawa, K. Wakui, G. Sawada, K. Sato, S. Matsuo, N. Yamaoka, *Catal. Surv. Jpn.* **2000**, *4*, 157–167.
[9] X. Liu, W. Li, H. Xu, Y. Chen, *React. Kinet. Catal. Lett.* **2004**, *81*, 203–209.
[10] X. Liu, W. Li, H. Zhu, Q. Ge, Y. Chen, H. Xu, *Catal. Lett.* **2004**, *94*, 31–36.
[11] K. Sundaram, G. F. Froment, *Ind. Eng. Chem. Fundam.* **1978**, *17*, 174–182.
[12] L. Leveles, K. Seshan, J. A. Lercher, L. Lefferts, *J. Catal.* **2003**, *218*, 296–306.

[13] L. Leveles, K. Seshan, J. A. Lercher, L. Lefferts, *J. Catal.* **2003**, *218*, 307–314.
[14] C. A. Boyadjian, L. Lefferts, K. Seshan, *Appl. Catal. A* **2010**, *372*, 167–174.
[15] C. A. Boyadjian, B. van der Veer, I. V. Babich, L. Lefferts, K. Seshan, *Catal. Today* **2010**, *157*, 345–350.
[16] C. Boyadjian, K. Seshan, L. Lefferts, A. G. J. van der Ham, H. van den Berg, *Ind. Eng. Chem. Res.* **2011**, *50*, 342–351.
[17] J.-P. Lange, R. J. Schoonebeek, P. D. L. Mercera, F. W. van Breukelen, *Appl. Catal. A* **2005**, *283*, 243–253.
[18] L. Leveles, S. Fuchs, K. Seshan, J. A. Lercher, L. Lefferts, *Appl. Catal. A* **2002**, *227*, 287–297.
[19] S. Gaab, J. Find, R. K. Grasselli, J. A. Lercher, *Stud. Surf. Sci. Catal.* **2004**, *147*, 673–678.
[20] M. V. Landau, M. L. Kaliya, A. Gutman, L. O. Kogan, M. Herskowitz, P. F. van den Oosterkamp, *Stud. Surf. Sci. Catal.* **1997**, *110*, 315–326.
[21] W. Yi-min, L. Shuo, L. Chun-yi, *J. Fuel Chem. Technol.* **2016**, *44*, 1334–1340.
[22] K. Otsuka, *Sekiyu Gakkaishi* **1987**, *30*, 385–396.
[23] K. Otsuka, K. Jinno, A. Morikawa, *Chem. Lett.* **1985**, *23*, 499.
[24] M. Nakamura, S. Takenaka, I. Yamanaka, K. Otsuka, *Stud. Surf. Sci. Catal.* **2000**, *130*, 1781–1786.
[25] E. M. Kennedy, N. W. Cant, *Appl. Catal.* **1991**, *75*, 321.
[26] J. Sa, M. Ace, J. J. Delgado, A. Goguet, C. Hardacre, K. Morgan, *ChemCatChem* **2011**, *3*, 394–398.
[27] K. Narasimharao, T. T. Ali, *Catal. Lett.* **2013**, *143*, 1074–1084.
[28] M. L. Kaliya, S. B. Kogan, N. Froumin, M. Herskowitz, *Catal. Commun.* **2002**, *3*, 327–333.
[29] M. L. Kaliya, S. B. Kogan, *Catal. Today* **2005**, *106*, 95–98.
[30] O. V. Buyevskaya, D. Mialler, I. Pitsch, M. Baerns, *Stud. Surf. Sci. Catal.* **1998**, *119*, 671–676.
[31] O. V. Buyevskaya, M. Kubik, M. Baerns, *ACS Symp., Ser.* **1996**, *638*, 155.
[32] O. V. Buyevskaya, M. Baerns, *Catal. Today* **1998**, *42*, 315–323.
[33] N. Kijima, K. Matano, M. Saito, T. Oikawa, T. Konishi, H. Yasuda, T. Sato, Y. Yoshimura, *Appl. Catal. A* **2001**, *206*, 237–244.
[34] F. Cavani, F. Trifiro, *Catal. Today* **1995**, *24*, 307–313.
[35] F. Cavani, F. Trifiro, *Appl. Catal. A* **1997**, *157*, 195–221.
[36] F. Cavani, F. Trifiro, *Catal. Today* **1997**, *36*, 431–439.
[37] F. Cavani, F. Trifiro, *Catal. Today* **1999**, *51*, 561–580.
[38] F. Cavani, N. Ballarini, A. Cericola, *Catal. Today* **2007**, *127*, 113.
[39] E. Heracleous, M. Machli, A. A. Lemonidou, I. A. Vasalos, *J. Mol. Catal. A* **2005**, *232*, 29–39.
[40] A. Christodoulakis, E. Heracleous, A. A. Lemonidou, S. Boghosian, *J. Catal.* **2006**, *242*, 16–25.
[41] A. Agiral, C. Trionfetti, L. Lefferts, K. Seshan, J. G. E. Gardeniers, *Chem. Eng. Technol.* **2008**, *31*, 1116–1123.
[42] C. Trionfetti, A. Agiral, J. G. E. Gardeniers, L. Lefferts, K. Seshan, *J. Phys. Chem. C* **2008**, *112*, 4267–4274.
[43] C. Trionfetti, A. Agiral, J. G. E. Gardeniers, L. Lefferts, K. Seshan, *ChemPhysChem* **2008**, *9*, 533–537.
[44] A. Agiral, C. Boyadjian, K. Seshan, L. Lefferts, J. G. E. Gardeniers, *J. Phys. Chem. A* **2010**, *114*, 18903–18910.
[45] C. Boyadjian, A. Agiral, J. G. E. Gardeniers, L. Lefferts, K. Seshan, *Plasma Chem. Plasma Process.* **2011**, *31*, 291–306.
[46] M. Huff, L. D. Schmidt, *J. Catal.* **1994**, *149*, 127–141.
[47] M. Huff, P. M. Torniainen, L. D. Schmidt, *Catal. Today* **1994**, *21*, 113–128.
[48] M. Huff, P. M. Torniainen, D. A. Hickman, L. D. Schmidt, *Nat. Gas Conv. II* **1994**, *81*, 315–320.
[49] L. D. Schmidt, M. Huff, *Catal. Today* **1994**, *21*, 443–454.
[50] S. S. Bharadwaj, L. D. Schmidt, *J. Catal.* **1995**, *155*, 403–413.
[51] A. G. Dietz III, A. F. Carlsson, L. D. Schmidt, *J. Catal.* **1998**, *176*, 459–473.
[52] S. S. Bharadwaj, C. Yokoyama, L. D. Schmidt, *Appl. Catal. A* **1996**, *140*, 73–97.
[53] J. J. Krummenacher, K. N. West, L. D. Schmidt, *J. Catal.* **2003**, *215*, 332–343.
[54] R. Subramanian, G. J. Panuccio, J. J. Krummenacher, I. C. Leeb, L. D. Schmidt, *Chem. Eng. Sci.* **2004**, *59*, 5501–5507.
[55] T. Berger, J. Schuh, M. Sterrer, O. Diwald, E. Knözinger, *J. Catal.* **2007**, *247*, 61–67.
[56] U. Zavyalova, M. Geske, R. Horn, G. Weinberg, W. Frandsen, M. Schuster, R. Schlögl, *ChemCatChem* **2011**, *3*, 949–959.
[57] K. Kwapien, J. Paier, J. Sauer, M. Geske, U. Zavyalova, R. Horn, P. Schwach, A. Trunschke, R. Schlögl, *Angew. Chem. Int. Ed.* **2014**, *53*, 8774–8778; *Angew. Chem.* **2014**, *126*, 8919.
[58] T. Ito, J.-X. Wang, C.-H. Lin, J. H. Lunsford, *J. Am. Chem. Soc.* **1985**, *107*, 5062–5068.
[59] M. Xu, C. Shi, X. Yang, M. P. Rosynek, J. H. Lunsford, *J. Phys. Chem.* **1992**, *96*, 6395–6405.
[60] E. Morales, J. H. Lunsford, *J. Catal.* **1989**, *118*, 255–265.
[61] S. J. Korf, J. A. Roos, N. A. de Bruijn, J. G. van Ommen, J. R. H. Ross, *Catal. Today* **1988**, *2*, 535–545.
[62] J. A. Roos, S. J. Korf, R. H. J. Veehof, J. G. Van Ommen, J. R. H. Ross, *Appl. Catal.* **1989**, *52*, 131–145.
[63] J. A. Roos, S. J. Korf, R. H. J. Veehof, J. G. van Ommen, J. R. H. Ross, *Catal. Today* **1989**, *4*, 441–452.
[64] M. Sterrer, T. Berger, O. Diwald, E. Knozinger, *J. Am. Chem. Soc.* **2003**, *125*, 195–199.
[65] R. Echterhoff, E. Knozinger, *Surf. Sci.* **1990**, *230*, 237–244.
[66] P. Schwach, W. Frandsen, M.-G. Willinger, R. Schlögl, A. Trunschke, *J. Catal.* **2015**, *329*, 560–573.
[67] P. Schwach, N. Hamilton, M. Eichelbaum, L. Thum, T. Lunkenbein, R. Schlögl, A. Trunschke, *J. Catal.* **2015**, *329*, 574–587.
[68] C. Trionfetti, I. V. Babich, K. Seshan, L. Lefferts, *Appl. Catal. A* **2006**, *310*, 105–113.
[69] C. Trionfetti, I. V. Babich, K. Seshan, L. Lefferts, *Langmuir* **2008**, *24*, 8220–8228.
[70] M. M. Abraham, Y. Chen, L. A. Boatner, R. W. Reynolds, *Phys. Rev. Lett.* **1976**, *37*, 849–852.
[71] Y. Chen, H. T. Tohver, J. Naraykn, M. M. Abraham, *Phys. Rev. B* **1977**, *16*, 5535–5542.
[72] M. Y. Sinev, V. Y. Bychkov, *Kinet. Katal.* **1993**, *34*, 309–316.
[73] M. Y. Sinev, V. Y. Bychkov, V. N. Korchak, E. L. Aptekar, O. V. Krylov, *Kinet. Catal.* **1989**, *30*, 1236–1242.
[74] M. A. Johnson, E. V. Stefanovich, T. N. Truong, *J. Phys. Chem. B* **1997**, *101*, 3196–3201.
[75] K.-I. Aika, J. H. Lunsford, *J. Phys. Chem.* **1977**, *81*, 1393–1398.
[76] K. T. Nguyen, H. H. Kung, *J. Catal.* **1990**, *122*, 415–428.
[77] S. Ahmed, A. Aitani, F. Rahman, A. Al-Dawood, F. Al-Muhaish, *Appl. Catal. A* **2009**, *359*, 1–24.
[78] E. C. Neyts, A. Bogaerts, *J. Phys. D* **2014**, *47*, 224010–224028.
[79] E. C. Neyts, K. Ostrikov, M. K. Sunkara, A. Bogaerts, *Chem. Rev.* **2015**, *115*, 13408–13446.
[80] B. Azambre, L. Zenboury, J. V. Weber, P. Burg, *Appl. Surf. Sci.* **2010**, *256*, 4570–4581.
[81] M. L. Rodriguez, D. E. Ardissone, E. Heracleous, A. A. Lemonidou, E. Lopez, M. N. Pedernera, D. O. Borio, *Ind. Eng. Chem. Res.* **2009**, *48*, 1090–1095.
[82] D. Ahchieva, M. Peglow, S. Heinrich, L. Mörl, T. Wolff, F. Klose, *Appl. Catal. A* **2005**, *296*, 176–185.

Received: October 27, 2017

